J. Synchrotron Rad. (1998). **5**, 406–408

SPring-8 in-vacuum undulator beam test at the ESRF

T. Hara,[a]* T. Tanaka,[a] T. Tanabe,[a] X.-M. Maréchal,[a] H. Kitamura,[a] P. Elleaume,[a] B. Morrison,[b] J. Chavanne,[b] P. Van Vaerenbergh[b] and D. Schmidt[b]

[a]SPring-8, Kamigori-cho, Ako-gun, Hyogo-ken 678-12, Japan, and [b]European Synchrotron Radiation Facility, BP 220, 38043 Grenoble CEDEX, France.
E-mail: toru@spring8.or.jp

(*Received 4 August 1997; accepted 21 October 1997*)

Before the commissioning of SPring-8, the in-vacuum hybrid undulator developed at SPring-8 had been brought to the ESRF for the first beam test in the summer of 1996. The purpose of this test was to investigate the influence of the in-vacuum undulator on the beam and check its vacuum system. However, heating by the resistive wall impedance turned out to be a critical issue for the in-vacuum undulators.

Keywords: undulators; in-vacuum undulators; resistive wall impedances.

1. Introduction

Before the commissioning of SPring-8, the first beam test of the SPring-8 in-vacuum undulator had been carried out at the ESRF using a 1.5 m segment of the hybrid-type in-vacuum undulator. It was installed in a low-β straight section (ESRF ID23, $\beta_x = 0.9$ m, $\beta_y = 3.5$ m). The main parameters of this undulator are given in Table 1.

The undulator vacuum system consists of two ion pumps ($125\ \mathrm{l\ s^{-1}} \times 2$) and four NEG pumps ($500\ \mathrm{l\ s^{-1}} \times 4$). TiN (5 µm thickness) is plated onto the magnet blacks to prevent out-gas and oxidation. In the off-line vacuum test, 3.0×10^{-8} Pa was achieved, and no vacuum problem was found during ring operation.

In order to decrease the beam impedance, the surface of the magnet array is covered with a metal sheet (50 µm thickness) (Hara *et al.*, 1998) and RF fingers connect between the ends of the magnet array and the adjacent vacuum ducts. Since the magnets are almost thermally isolated in the vacuum, water cooling is provided to the magnets during ring operation to prevent a temperature rise. These magnet sheets and the RF fingers produce a gentle transition of the cross section and a smooth surface for the electron beam.

2. Closed-orbit distortion as a function of the undulator gap

The error of the integrated magnetic field produces a kick on the electron beam at the undulator, resulting in a closed-orbit distortion (COD) around the ring. Generally speaking, this integrated field error varies with the undulator gap. To minimize this effect, the magnetic field is corrected by inserting small magnet chips on the back of the magnets. Fig. 1 shows the measured COD as a function of the undulator gap. It agrees with the expected one from the magnetic field measurement. In order to cancel the remaining integrated field error, long coils, whose current changes with the gap, are used at SPring-8, and the COD change is suppressed within 10% of the beam size (Hara *et al.*, 1998; Kitamura, 1998).

Table 1
Main parameters of the in-vacuum hybrid undulator.

Type	Hybrid device
Length	1.5 m (1/3 of the SPring-8 standard-type in-vacuum undulator)
Number of periods	62
Period length	24 mm
Magnet sheet	50 µm stainless steel (SUS)
RF fingers	0.25 mm BeCu (C1720)

3. Resistive wall heating in the in-vacuum undulator

The most serious trouble experienced at the ESRF was the heating due to the resistive wall impedance (Bane & Krinsky, 1993). At the first stage of the in-vacuum undulator development, a 50 µm SUS (stainless steel) sheet was used as the magnet sheet. When the gap was closed, the electron beam was lost partially or totally under a gap of 8–9 mm. The temperature of the RF fingers also rose to 473 K. These phenomena seemed to be more significant for higher peak currents.

The reason for the beam loss was not clear at the time of the beam test. However, after opening the vacuum chamber we found that the SUS magnet sheet was fused, as shown in Fig. 2. The fused part is at the entrance of the undulator and the outer side of the ring. From this, we concluded that the sheet was heated by the resistive wall effect, and the thermal expansion of the sheet resulted in detachment of the sheet from the magnet

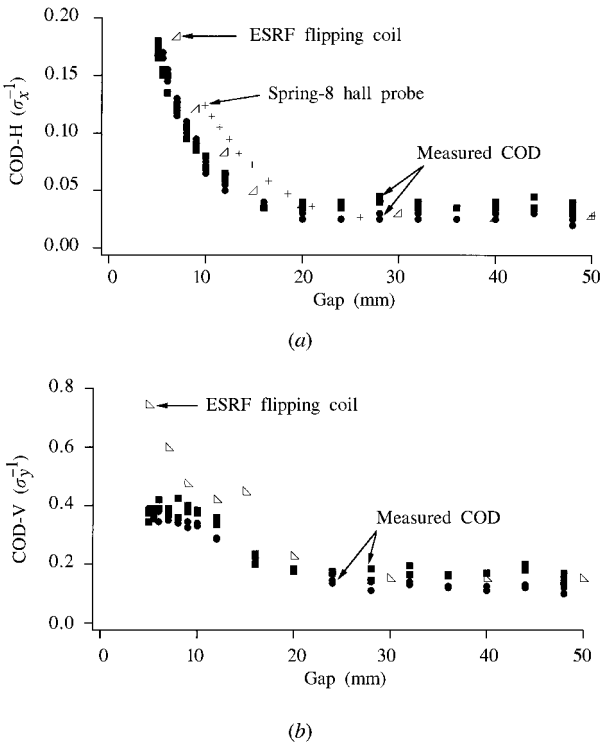

Figure 1
Measured and expected COD as a function of the undulator gap, normalized by the beam size. (*a*) Horizontal, (*b*) vertical.

Table 2
Power of the resistive wall heating calculated for the 1.5 m in-vacuum undulator at ESRF.

	Beam mode	Average current (mA)	Bunch length, σ_t (ps)	Material	Power (W m^{-1})
Magnet sheet gap 5 mm	1/3 filling (300 bunches)	140	15	SUS	28
				Ni + Cu	4.4
	16 bunches	90	35	SUS	61
				Ni + Cu	9.6
RF finger gap 5 mm	1/3 filling (300 bunches)	140	15	BeCu	2.2
	16 bunches	90	35	BeCu	4.8

surface. Once the thermal contact between the sheet and the magnets was lost, it accelerated the temperature rise and the deformation of the sheet. Finally, the synchrotron radiation from the bending magnet immediately before the undulator hit and fused the sheet. Due to gravity, the sheet on the upper magnets was seriously damaged, but there was only one small melted spot on the lower sheet. The amount of power, P, produced by the resistive wall impedance has the relation

$$P \propto MI_{\rm peak}^2/g\rho^{1/2},$$

where M, $I_{\rm peak}$ and g are the number of bunches, the peak current and the undulator gap, respectively, and ρ is the electrical conductivity of the sheet material (Bane & Krinsky, 1993). Table 2 shows the estimation of the power due to the resistive wall effect. Even if the power is not so large, the thermal deformation of the sheet could be a serious problem.

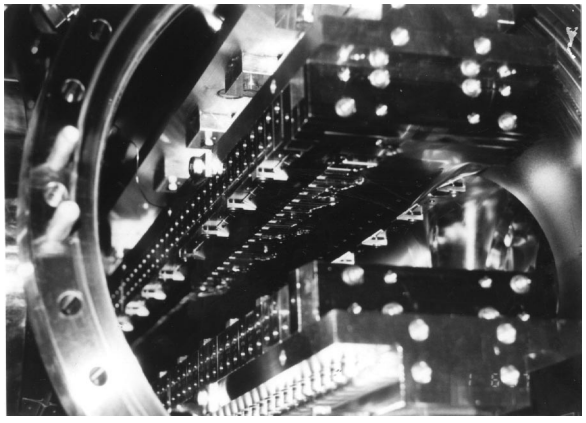

Figure 2
The fused magnet sheet after the test.

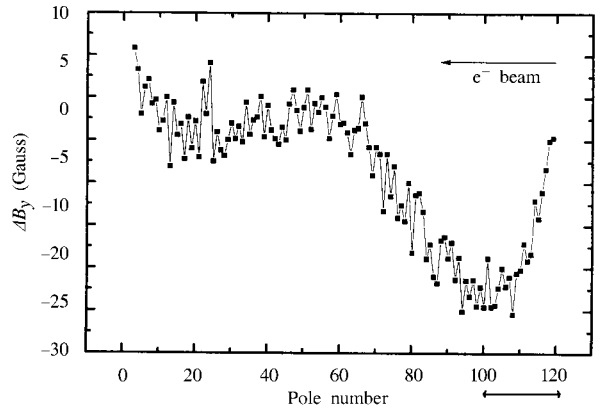

Figure 3
Demagnetization of the undulator field (gap = 9.7 mm). The arrow on the x axis shows where the SUS sheet was fused, *i.e.* between poles 100 and 120.

The magnetic field of the undulator was remeasured after the test; the field change during the beam test is plotted in Fig. 3. The electron beam enters the undulator from the right-hand side in Fig. 3, and the sheet was fused between the pole numbers 100 and 120. The peak field of a 9.7 mm gap is about 4600 G, so a demagnetization of 0.5% is observed between the pole numbers 70 and 120. The magnet temperature was measured at the side face of the magnet holders. Since the magnet temperature was always constant during the beam test and the demagnetized part extends downstream compared with the fused area, the demagnetization is thought to be due to the electrons which are scattered by the fused sheet and hit the magnet. Even if the sheet is floated from the magnets only by a few millimetres, the sheet is isolated thermally and the synchrotron radiation power is absorbed at a very local area on the sheet.

4. Improvements

To avoid the resistive wall heating problem, improvements of the magnet sheet material and the RF fingers were included in the new designs for the SPring-8 in-vacuum undulators.

The SUS magnet sheet was replaced by a Cu (10 µm)-coated Ni (50 µm) sheet, which has better electrical and thermal conductivity; thus, the heat production is reduced by more than one-sixth compared with the SUS sheet (Table 2), and the temperature rise should decrease further. The power spectrum of the resistive wall heating (Bane & Krinsky, 1993) is plotted in Fig. 4. The integration of Fig. 4 is equal to the total power. From this figure, it can be seen that 10 µm Cu is thick enough compared with infinite Cu. Another important feature of the new sheet is the use of Ni. Since Ni possesses magnetism, thermal contact between the magnets and the sheet is ensured. The flux loss due to the Ni sheet is less than 0.1% of the undulator field; therefore it is negligible.

The material of the RF finger was also changed, to high electrical and thermal conductive BeCu, and its holders were changed from SUS to Cu. In addition, a water-cooling channel was supplied to take out the heat. A photograph of the new RF finger for the SPring-8 in-vacuum undulators is shown in Fig. 5. The face with the elliptical aperture is connected to the ring vacuum ducts.

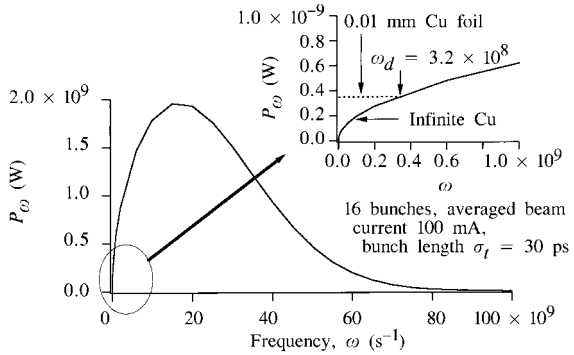

Figure 4
Power spectrum of the resistive wall heating.

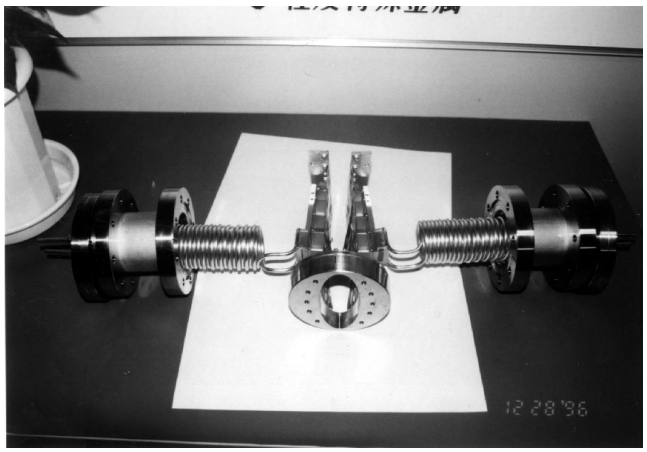

Figure 5
New RF finger for the SPring-8 in-vacuum undulators.

The water-cooling Cu tube forms a spiral to follow the gap movement.

5. Conclusions

One of the important issues of the in-vacuum undulators is the resistive wall heating. Differing from a smooth vacuum duct of conventional out-vacuum undulators, the surfaces seen by the electron beam have various structures in the in-vacuum undulators, such as the magnets, the RF fingers *etc.* These structures are almost thermally isolated in the vacuum and the electron beam passes nearby. Thus, careful attention should be paid to their design.

Except for the resistive wall problem, the in-vacuum undulator performed well during the ESRF beam test. During the commissioning of SPring-8, no serious problems concerning the resistive wall effect have been met so far.

References

Bane, K. & Krinsky, S. (1993). *Proc. 1993 IEEE Part. Accel. Conf.*, pp. 3375–3377. IEEE Service Center, NJ, USA.
Hara, T., Tanaka, T., Tanabe, T., Maréchal, X.-M., Okada, S. & Kitamura, H. (1998). *J. Synchrotron Rad.* **5**, 403–405.
Kitamura, H. (1998). *J. Synchrotron Rad.* **5**, 184–188.